Global NEST Journal, Vol 23, No 3, pp 475-482

Analysis of regional heavy $PM_{2.5}$ pollution events in Beijing-Tianjin-Hebei and the surrounding area in China during 2015–2018

Wang Z.[1+], Qian Y.[1+], Li Z.[1], Wu K.[2,3], Guo C.[1], Zhang L.[4+], Li X.[1]* and Guo J.[5]

[1]State Key Laboratory of Environmental Criteria and Risk Assessment, Chinese Research Academy of Environmental Sciences, Beijing, China

[2]Plateau Atmosphere and Environment Key Laboratory of Sichuan Province, School of Atmospheric Sciences, Chengdu University of Information Technology, Chengdu, China

[3]Department of Land, Air, and Water Resources, University of California, Davis, CA, USA

[4]Center for Environmental Emergency and Heavy Pollution Early Warning, Hebei Environmental Protection Bureau, Shijiazhuang, China

[5]Jinan Environmental Research Institute, Jinan 250101, China

[+]These authors contributed equally to this work.

Received: 08/03/2021, Accepted: 01/11/2021, Available online: 04/11/2021

*to whom all correspondence should be addressed: e-mail: hkyzkjh@sina.com, qingkongweilan@tom.com

https://doi.org/10.30955/gnj.003589

Graphical abstract

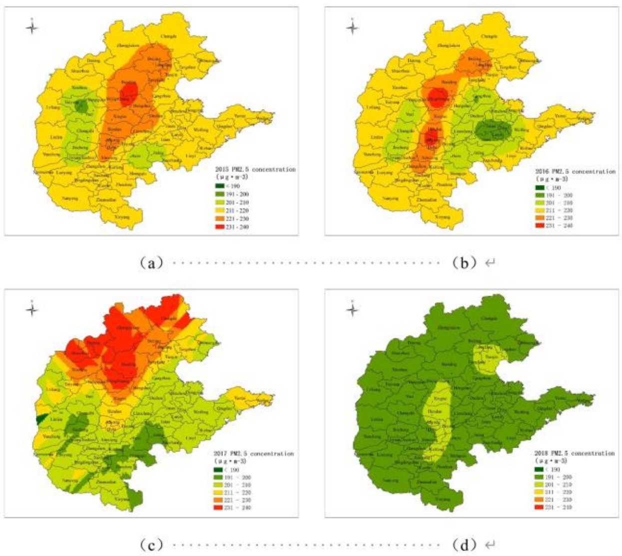

Abstract

Beijing-Tianjin-Hebei and the surrounding area (BTHS) experiences the most serious $PM_{2.5}$ pollution in China. To investigate $PM_{2.5}$ pollution characteristics in regional heavy air pollution, forty-three events in BTHS during 2015–2018 were selected in this study. These regional events generally lasted five days and covered nineteen cities, with an average $PM_{2.5}$ concentration of 204 μg·m^{-3} and a maximum daily average concentration of 358 μg·m^{-3}. The pollution events occurred mainly during October to March of the following year, which is the heating season in this region. The occurrence of pollution events and the $PM_{2.5}$ concentration displayed a decreasing trend during 2015–2018. Of the forty-three events, thirteen started in Baoding city, and the peak $PM_{2.5}$ concentration was recorded in Baoding city eleven times, indicating that it was the most polluted city in BTHS. A comprehensive classification method determined that southwest channel pollution was the main type of pollution event in BTHS. It occurred nine, seven, four, and eight times in 2015–2018, accounting for 56.3%, 53.8% 80.0%, and 88.9% of all pollution events, respectively. A typical regional heavy $PM_{2.5}$ pollution event occurred in March 2016. The analysis revealed that it was initiated by pollutant transport from regions south of BTHS. Local pollutant emissions and regional pollutants accumulated, and secondary pollutant formation occurred in association with weak winds and a high relative humidity, which maintained the heavy pollution levels. Relative humidity had the most significant influence on the two most important stages of a heavy $PM_{2.5}$ pollution event, which were the initial and high concentration stages, respectively.

Keywords : Beijing-Tianjin-Hebei region; $PM_{2.5}$ pollution; spatial-temporal characteristics; classification; relative humidity.

1. Introduction

With rapid industrialization and urbanization, and the continuous increase in energy consumption, air pollution has become serious in China during recent years (Cheng *et al.*, 2019; Ding *et al.*, 2019; Hou *et al.*, 2019; Ji *et al.*, 2018; Li *et al.*, 2020). Regional air pollutants, particularly $PM_{2.5}$, have become the main factor restricting the improvement of environmental quality in China (Gong *et al.*, 2019; Ji *et al.*, 2019; Wang *et al.*, 2015a; Wang *et al.*, 2019; Yan *et al.*, 2018; Yu *et al.*, 2014).

Beijing-Tian-Hebei and the surrounding area (BTHS) is one of the most $PM_{2.5}$-polluted areas in China. Geographically, BTHS is located in the north of the North China Plain, with the Yanshan Mountains to the north, the Taihang Mountains to the west, and Bohai Bay to the east. The region consists of semi-enclosed topographic features, with a high elevation in the northwest and a low elevation in the southeast; thus, air pollutants can easily accumulate in this area. In terms of meteorological conditions, BTHS is dry and rainless, leading to weak wet deposition of air pollutants. The mountains in the northwest weaken the pollution-removal effect of the northwest monsoon that prevails in winter, and therefore the diffusion of air pollutants is relatively poor in BTHS. In addition, air pollutant emissions are high due to the heavy industry-based industrial structure, coal-based energy structure, and highway-based traffic structure (Ye *et al*., 2019; Yi *et al*., 2018; Wu *et al*., 2018b).

Studies of $PM_{2.5}$ pollution in BTHS have been conducted during recent years. Some studies have revealed the temporal–spatial characteristics of $PM_{2.5}$ in different years (He *et al*., 2020; Hu *et al*., 2014; Lei *et al*., 2016; Xue *et al*., 2019Zhao *et al*., 2017). Other studies have focused on the source apportionment of air pollutants in this region (Chen *et al*., 2017; Wang *et al*., 2015b; Zhang *et al*., 2017; Zhu *et al*., 2019). The health effects of $PM_{2.5}$ have also been investigated (Feng, 2017; Li *et al*., 2019; Song *et al*., 2011; Yang, 2020; Zhao *et al*., 2019; Zheng *et al*., 2019), while some studies have assessed the effects of long-term and temporary measures to reduce air pollutant emissions (Guo *et al*., 2018; Wang *et al*., 2016, 2018).

However, most of those previous studies were limited to few sampling locations or a short sampling period. In this study, $PM_{2.5}$ monitoring data from twenty-seven cities in BTHS during a 4-year period (2015–2018) were analyzed. The main objectives of the study were to (1) define and identify regional heavy $PM_{2.5}$ pollution events in BTHS, (2) characterize the spatial and temporal variations in $PM_{2.5}$ concentrations in regional heavy air pollution, (3) determine a classification system for regional heavy $PM_{2.5}$ pollution events in BTHS, and (4) analyze typical $PM_{2.5}$ pollution events in BTHS.

2. Data collection and analysis method

Twenty-seven cities in BTHS were selected (Figure 1). For each city, $PM_{2.5}$ data were obtained from the China National Environmental Monitoring Center (http://www.cnemc.cn/). Quality assurance and quality control of $PM_{2.5}$ data followed the Ambient Air Quality Standards (GB3095-2012) and Technical Regulation on Ambient Air Quality Index (on trial) (HJ 633-2012). Meteorological data and $PM_{2.5}$ chemical composition were obtained for the analysis of typical $PM_{2.5}$ pollution events. Meteorological data from the Guanxiangtai site was obtained from the National Meteorological Information Center (http://data.cma.cn).

The $PM_{2.5}$ chemical composition was observed at the Langfang Municipal Ecology and Environment Bureau (LFMEEU), which is located 10 km outside of Beijing (Figure 1). Organic carbon (OC) and elemental carbon were measured using the RT-4 analyzer (Sunset Lab Inc., Portland, OR, USA). Water-soluble cations and anions were measured by ICS-2000 and ICS-3000 ion chromatographic analyzers, respectively (Dionex, Sunnyvale, CA, USA). To ensure the validity and accuracy of the monitoring data, all monitoring instruments were calibrated regularly according to national standards. Volatile organic compounds were removed by inline parallel carbon denuder removing installed on the analyzer. Round 16-mm quartz filters were used for collecting OC and EC samples at a sampling flow rate of 8 L/min. OC and EC samples were collected for 40min and then were analyzed in approximately 15 min. The multiple programmed steps were based on the NIOSH 5040 thermal protocol. A non-dispersive infrared (NDIR) detector was used for quantifying particulate OC and EC concentrations.

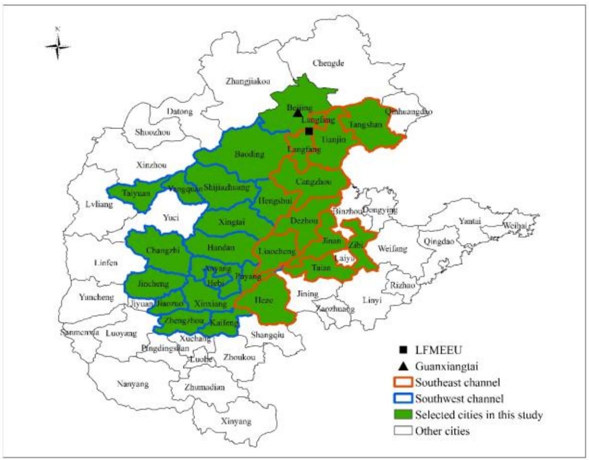

Figure 1. The twenty-seven selected cities (green) and the monitoring sites used in this study. Meteorological data were observed in Guanxiangtai, and the chemical composition of $PM_{2.5}$ was observed at the Langfang Municipal Ecology and Environment Bureau (LFMEEU). Cities with red border referred to cities in the southeast transport channel and cities with blue border referred to cities in the southwest transport channel.

The kriging method was selected to obtain the spatial characteristics of $PM_{2.5}$ in BTHS. As one of main contents of geostatistics, kriging interpolation is a method of unbiased optimal estimation for regionalized variables, which is based on variation function theory and structural analysis. Kriging model mainly uses variograms of geographic factors and the structural characteristics of the original data to perform unbiased and linear optimal interpolation estimation of spatial variables. This model can overcome the problem that the interpolation error is difficult to analyze, can theoretically estimate the error point by point, and will not produce the boundary effect of regression analysis. It is an unbiased estimation method of spatial interpolation (Hough *et al*., 2020; Jin *et al*., 2019; Pan *et al*., 2019; Tayaran *et al*., 2019). The formula for kriging model is

$$Z(X)=\sum_{i=1}^{n}\lambda Z_i$$

where Z(X) is the estimated value at X; n is the number of monitoring sites; λ is the kriging weight; and Z_i is the measured value at X_i.

3. Results and discussion

3.1. Definition of regional heavy $PM_{2.5}$ pollution events

According to the definition used by the China National Environmental Monitoring Centre, when the daily average $PM_{2.5}$ concentration in three or more of the twenty-seven cities reached 150 $\mu g{\cdot}m^{-3}$ for three or more days, the pollution episode was classified as a regional heavy $PM_{2.5}$ pollution event. Forty-three such events were detected during 2015–2018, as shown in Table S1 in supplementary material. Start city refers to the city with the highest $PM_{2.5}$ concentration on the day that the regional heavy $PM_{2.5}$ pollution event began. In general, regional heavy $PM_{2.5}$ pollution events, with an average $PM_{2.5}$ concentration of 204 $\mu g{\cdot}m^{-3}$ and maximum daily average $PM_{2.5}$ concentration of 358 $\mu g{\cdot}m^{-3}$, lasted five days. On average, nineteen cities were affected by one regional heavy $PM_{2.5}$ pollution event. Thus, regional pollution events resulted in serious $PM_{2.5}$ pollution conditions.

Table 1. Descriptive statistics of regional heavy $PM_{2.5}$ pollution events in individual cities

City	Frequency of being the start city				
	2015	**2016**	**2017**	**2018**	**Total**
Baoding	7	3	2	1	13
Zhengzhou	2				2
Beijing	1				1
Beijing	1	1			2
Liaocheng	1				1
Dezhou	1				1
Jinan	1				1
Shijiazhuang	1	2		1	4
Puyang	1			1	2
Handan	1	1	1		3
Anyang		2	1	2	5
Xinxiang		2			2
Tangshan		1			1
Taiyuan		2	1		3
Hengshui				1	1
Kaifeng				1	1
Heze				1	1
City	**Frequency of being the city with the peak PM2.5 concentration**				
	2015	**2016**	**2017**	**2018**	**Total**
Anyang	4	1	1	3	9
Baoding	5	3	2	1	11
Liaocheng	1				1
Jiaozuo	1	1			2
Xingtai	1			1	2
Langfang	1				1
Beijing	2	2		1	5
Hengshui	1				1
Xinxiang	1				1
Dezhou		1			1
Changzhi		1			1
Taiyuan		2			2
Shijiazhuang		2	2	2	6
Handan		1			1
Kaifeng				1	1

3.2. Temporal characteristics of regional heavy $PM_{2.5}$ pollution events

Regional heavy $PM_{2.5}$ pollution events occurred sixteen, thirteen, five, and nine times from 2015 to 2018, respectively, indicating a decreasing trend, with a rebound in 2018. These events occurred mainly during October to March of the following year, which is the heating season in this region. The period between April and September was typically a clean period without any regional heavy $PM_{2.5}$ pollution events. During the clean period, air pollutant emission is lower and atmospheric pollution diffusion condition is more favorable than other time period. In general, these events lasted for five, five, eight, and five days during 2015–2018, respectively. In 2017, these events occurred the least frequently but lasted longer than those during other years. The events took two, two, three, and two days to reach the $PM_{2.5}$ concentration peak during 2015–2018, respectively. The average $PM_{2.5}$ concentrations in these events were 211, 196, 215, and 196 µg·m^{-3}, respectively. The maximum $PM_{2.5}$ concentrations in these events were 374, 345, 416, and 308 µg·m^{-3}, respectively, indicating a decreasing trend, with a rebound in 2017. In general, the occurrence and $PM_{2.5}$ concentration displayed a decreasing trend during 2015–2018.

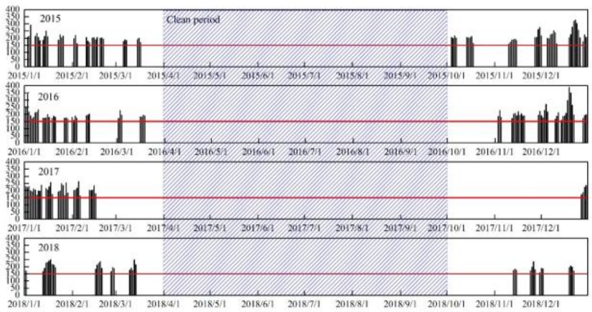

Figure 2. The average daily $PM_{2.5}$ concentrations in the twenty-seven cities during 2015–2018. The time from April to September was defined as a clean period, because no regional heavy $PM_{2.5}$ pollution events occurred.

3.3. Spatial characteristics of regional heavy $PM_{2.5}$ pollution events

Regional heavy $PM_{2.5}$ pollution events affected eighteen, seventeen, twenty-four, and twenty cities from 2015 to 2018, respectively. In 2017, the events occurred the least frequently but had the highest $PM_{2.5}$ concentration, lasted the longest duration, and affected the most cities. Table 1 shows the frequencies at which each city became the start city and had the peak concentration. Of the forty-three events, thirteen started in Baoding city, accounting for 30.2% of the events, followed by Anyang (five events), Shijiazhuang (five events), Handan (five events), and Taiyuan (five events). Of the twenty-seven cities, seventeen were the start city at some time (Figure 3). The peak $PM_{2.5}$ concentration was recorded eleven times in Baoding city, accounting for 25.6% of all peak concentrations, followed by Shijiazhuang (six times) and Beijing (five times). The peak $PM_{2.5}$ concentration was recorded in fifteen of the twenty-seven cities at some point during the study (Figure 3). In general, $PM_{2.5}$ pollution was most serious in Baoding and Shijiazhuang.

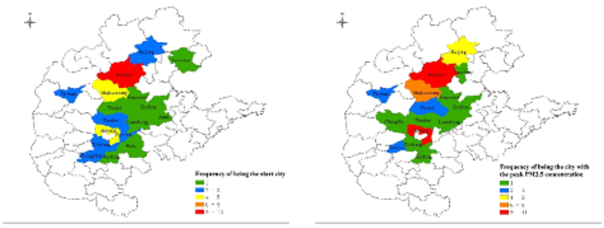

Figure 3. Frequency of being the start city and being the city with the peak $PM_{2.5}$ concentration in the forty-three events evaluated in Beijing-Tianjin-Hebei and the surrounding area (BTHS).

Figure 4 shows the spatial distribution of the $PM_{2.5}$ concentration based on the Kriging method (Jamil and Bellos, 2019; Ma *et al*., 2019; Wu *et al*., 2018a; Young *et al*., 2016) in regional heavy $PM_{2.5}$ pollution events during 2015–2018. In 2015, the region with the highest $PM_{2.5}$ concentration had a zonal distribution alongside the Taihang Mountains, affecting the cities of Beijing, Baoding, Langfang, Shijiazhuang, Hengshui, Xingtai, Handan, and Anyang. The $PM_{2.5}$ concentrations were highest in Baoding and Shijiazhuang. In 2016, the region with the highest $PM_{2.5}$ concentrations also had a zonal distribution, but the extent of the affected region decreased. The $PM_{2.5}$ concentrations were highest in Anyang and Shijiazhuang. In 2017, the spatial distribution changed, and the highest concentrations occurred in the northern area of BTHS, including Baoding, Shijiazhuang, and Beijing. In 2018, $PM_{2.5}$ concentrations were significantly lower than during the first three years. The $PM_{2.5}$ concentrations were higher in Tianjin and the southern region of the Taihang Mountains than elsewhere in the region. The spatial characteristics of $PM_{2.5}$ during the 4-year period also indicated that the air quality was improving.

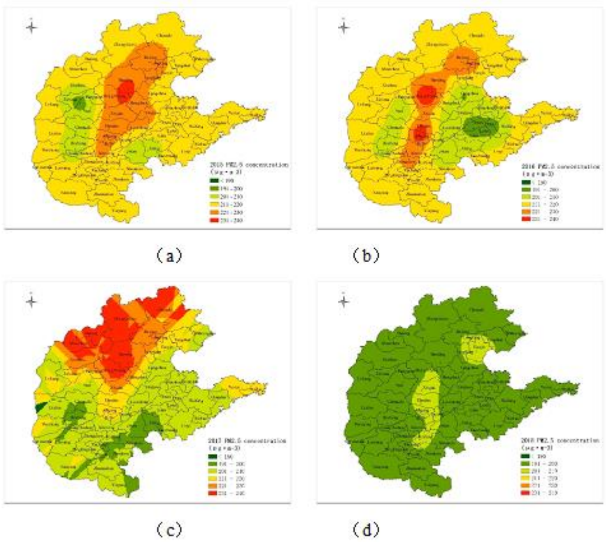

Figure 4. Spatial distribution of the $PM_{2.5}$ concentration during heavy $PM_{2.5}$ pollution events during 2015–2018.

3.4. Classification of regional heavy $PM_{2.5}$ pollution events

According to their geographical orientation and influence on Beijing, the twenty-seven cities were divided into two transmission channels, southwest and southeast channels, as shown in Figure 1.

Three methods were applied to classify the regional heavy $PM_{2.5}$ pollution events, with the preliminary results shown in Table 2. Based on the location of the start city and the city with the peak concentration, it was apparent that most events were of the southwest channel transmission type. According to the number of cities in the different channels, the results were different from those obtained using other methods. More events in 2015 and 2016 were of the southeast channel type, while most events in 2017 and 2018 were of the southwest channel type. A comprehensive classification method was developed based on this. If more than 80% of the affected cites were in one channel, then the event was defined as the corresponding channel type. Additionally, the classification was conducted according to the location of the start city. The final classification of the forty-three events is shown in Table S1. The southwest channel pollution type was the main type in BTHS; it occurred nine, seven, four, and eight times from 2015 to 2018, respectively, accounting for 56.3%, 53.8%, 80.0%, and 88.9% of all events.

Table 2. Preliminary classification of regional heavy $PM_{2.5}$ pollution events

Year	Start city		City with the peak concentration		Number of affected cities	
	Southwest	Southeast	Southwest	Southeast	Southwest	Southeast
2015	13	3	13	2	7	10
2016	12	1	11	1	5	8
2017	5	0	5	0	4	1
2018	7	1	8	0	7	1

Table 3. Meteorological data during different stages of the event

Stage	Surface pressure (hPa)	Temperature (°C)	Relative humidity (%)	Visibility (m)	Wind speed (m/s)	North wind frequency (%)
S1	1010.2	10.2	57.1	2840.9	1.7	4.5
S2	1008.1	10.9	56	1517.2	1.4	37.9
S3	1013.6	13.1	35.1	8571.1	2.4	57.8

3.5. Analysis of a typical regional heavy $PM_{2.5}$ pollution event

In March 2016, a 4-day regional heavy $PM_{2.5}$ pollution event occurred after the heating season. The event started on 16 March in Beijing and affected nineteen cities. The daily average $PM_{2.5}$ concentration was 186 $\mu g \cdot m^{-3}$, and the daily maximum $PM_{2.5}$ concentration was 288 $\mu g \cdot m^{-3}$. The peak concentration occurred in Beijing. Figure 5 shows the evolution of the $PM_{2.5}$ concentration in the nineteen cities. The event was divided into three stages: S1 (00:00–21:00 March 16), S2 (22:00 March 16 to 02:00 March 18), and S3 (03:00 March 18 to 23:00 March 19). At the beginning of S1, the $PM_{2.5}$ concentration in Beijing was at an intermediate level among the nineteen cities. On the afternoon of March 16, the $PM_{2.5}$ concentration increased rapidly in Beijing, which became the city with the highest $PM_{2.5}$ concentration in BTHS. The S1 stage involved the accumulation of pollutants and formation of the regional heavy $PM_{2.5}$ pollution event. In S2, the $PM_{2.5}$ concentration fluctuated but was maintained at the highest level in Beijing of all cities in BTHS. At the end of S2, the peak $PM_{2.5}$ concentration (358 $\mu g \cdot m^{-3}$) occurred in Beijing. A high $PM_{2.5}$ concentration was maintained throughout S2. During the first half of S3, the $PM_{2.5}$ concentration in Beijing decreased slowly but increased in other cities. Then, a large mass of cold air reached the area, and the $PM_{2.5}$ concentration in Beijing decreased rapidly. Cities in the northern area of BTHS were affected by the north wind, and the $PM_{2.5}$ concentration decreased to a low level. Cities in the southern part of BTHS were not affected by this cold air, and a high $PM_{2.5}$ concentration was maintained. The regional heavy $PM_{2.5}$ pollution event finally ended at the end of S3, which was considered the clean-up period.

Table 3 shows the meteorological data during the different stages. In S1, surface pressure was maintained at a low level, and relative humidity peaked at 57.1%. The wind was weak, with an average speed of 1.7 m/s, and the north wind frequency was only 4.5%. Thus, at the beginning of the event, Beijing was affected by regional transport caused by the persistent southerly wind. In S2, the surface pressure was lower, but the relative humidity was the same, compared with those in S1. Wind speed and visibility kept decreasing, indicating that meteorological conditions were more unfavorable. Although the north wind frequency increased, the wind was too weak to disperse the pollution. In S3, surface pressure, wind speed, and north wind frequency increased, whereas relative humidity decreased to a low level. Due to the arrival of a strong cold air mass, meteorological conditions became favorable, and the event ended.

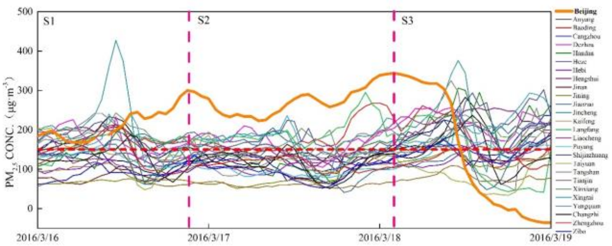

Figure 5. The evolution of the $PM_{2.5}$ concentration in the nineteen cities during this event. The time period S1–S3 refers to the different stages of the event.

Figure 6 shows the variation in the chemical composition of $PM_{2.5}$ during this event. The main chemical constituents of $PM_{2.5}$ were SO_4^{2-}, NO_3^-, NH^{4+}, and OC. The location where these samples were collected was 10 km from the border of Beijing and could therefore represent the pollution characteristics of Beijing during a large-scale regional heavy $PM_{2.5}$ pollution event. The SO_4^{2-}, NH^{4+}, and OC concentrations were similar. The NO_3^- concentration was highest during this event, indicating the contribution of local vehicle emissions. There were several sudden and rapid increases in the NO_3^- concentration, indicating that secondary chemical formation had a significant influence on the $PM_{2.5}$ concentrations during this event.

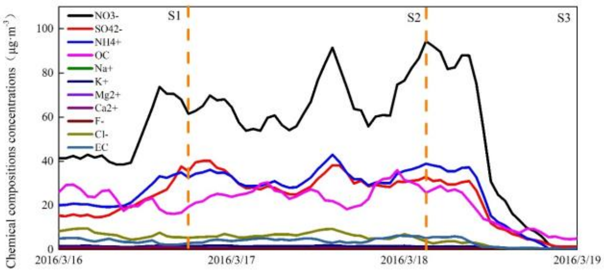

Figure 6. Variations in the chemical composition of $PM_{2.5}$ during this event.

In conclusion, this regional heavy $PM_{2.5}$ pollution event was caused by a combination of local pollutant emissions and regional pollutant transport under unfavorable meteorological conditions. Pollutant transport from regions south of BTHS initiated the heavy $PM_{2.5}$ pollution in Beijing. Local pollutant emissions and regional pollutants accumulated, and secondary chemical formation occurred, under conditions with weak wind and high relative humidity, which maintained the heavy pollution levels. Finally, the arrival of a strong cold air mass ended this event.

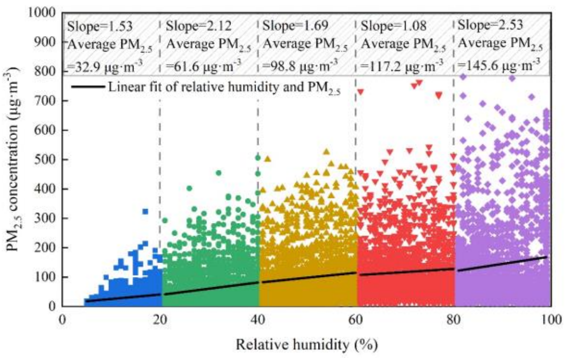

Figure 7. Correlation analysis of relative humidity and $PM_{2.5}$ in Beijing during 2013. The different colors refer to different relative humidity ranges, and the black line refers to the linear fit of relative humidity and $PM_{2.5}$ at different relative humidity ranges.

3.6. The relationship between $PM_{2.5}$ and relative humidity

As shown in Table 3, relative humidity and wind speed were the meteorological parameters that had the most significant influence on $PM_{2.5}$. For the horizontal transport of pollutants, wind from different directions had different effects on $PM_{2.5}$ (Chen *et al*., 2018, 2019; Liang *et al*., 2019; Liu and Ren, 2019; Xie *et al*., 2019; Yue *et al*., 2020; Zhang *et al*., 2020). Many studies have confirmed the unfavorable influence of relative humidity on $PM_{2.5}$ (Chen *et al*., 2015; Fu *et al*., 2016; Sun *et al*., 2020; Tai *et al*., 2010; Xie *et al*., 2020). The year 2013 was selected for analysis, because the most serious $PM_{2.5}$ pollution occurred during that year. Figure 7 shows the results of a correlation analysis of the relationship between relative humidity and $PM_{2.5}$. Relative humidity was divided into five ranges to investigate its relationship with the $PM_{2.5}$ concentration. At all ranges, the $PM_{2.5}$ concentration was positively correlated with relative humidity, indicating that an increase in relative humidity aggravated $PM_{2.5}$ pollution. According to the slopes in the five ranges, relative humidity ranges of 80–100% and 20–40% had the most significant influence on the $PM_{2.5}$ concentration. The average $PM_{2.5}$ concentrations within these ranges were 61.6 and 145.6 $\mu g{\cdot}m^{-3}$, respectively. According to the Technical Regulation on Ambient Air Quality Index (on trial), a daily average $PM_{2.5}$ concentration of 75 $\mu g{\cdot}m^{-3}$ is the air quality limit between good and mild pollution. A daily average $PM_{2.5}$ concentration of 150 $\mu g{\cdot}m^{-3}$ is the air quality limit between moderate and serious pollution. Thus, relative humidity had the most significant influence on the two most important stages of a heavy $PM_{2.5}$ pollution event, which were the initial and high concentration stages, respectively. Thus, relative humidity is one of the most important meteorological factors affecting $PM_{2.5}$ concentrations in Beijing.

4. Conclusion and suggestions

(1) A pollution episode was classified as a regional heavy $PM_{2.5}$ pollution event when daily average $PM_{2.5}$ concentrations in three or more of the twenty-seven cities reached 150 $\mu g{\cdot}m^{-3}$ for three or more days. Forty-three events were selected during 2015–2018. In general, regional heavy $PM_{2.5}$ pollution events lasted five days and covered nineteen cities with an average $PM_{2.5}$ concentration of 204 $\mu g{\cdot}m^{-3}$ and a maximum daily average $PM_{2.5}$ concentration of 358 $\mu g{\cdot}m^{-3}$.

(2) These events occurred mainly from October to March of the next year, which was the heating season in this region. The occurrence of pollution events and the $PM_{2.5}$ concentration displayed a decreasing trend during 2015–2018. Baoding experienced the beginning of thirteen events and the peak $PM_{2.5}$ concentration eleven times. Shijiazhuang experienced the beginning of five events in Shijiazhuang and the peak $PM_{2.5}$ concentration six times, indicating that Baoding and Shijiazhuang were the most polluted cities in BTHS.

(3) Three methods were applied to classify regional heavy $PM_{2.5}$ pollution events. A comprehensive classification method determined that southwest channel pollution was the main type of pollution event in BTHS. Southwest channel pollution occurred nine, seven, four, and eight times in 2015–2018, accounting for 56.3%, 53.8% 80.0%, and 88.9% of all pollution events, respectively.

(4) A typical regional heavy $PM_{2.5}$ pollution event, in which Beijing experienced the peak concentration, occurred in March 2016. An analysis of the pollutant characteristics was conducted based on the $PM_{2.5}$ concentration, meteorological data, and chemical composition of $PM_{2.5}$. The results showed that this event was caused by a combination of local pollutant emissions and regional pollutant transport under unfavorable meteorological conditions. According to a correlation analysis of the relative humidity and $PM_{2.5}$, relative humidity ranges of 80–100% and 20–40% had the most significant influence on the $PM_{2.5}$ concentration in Beijing.

Acknowledgments

This work was funded by the National Natural Science Foundation of China (No. 41705112).

References

Chen C., Cai J., Wang C., et al. (2018). Estimation of personal $PM_{2.5}$ and BC exposure by a modeling approach–Results of a panel study in Shanghai, China. *Environment international*, **118**, 194–202.

Chen D., Liu X., Lang J., et al. (2017). Estimating the contribution of regional transport to $PM_{2.5}$ air pollution in a rural area on the North China Plain. *Science of The Total Environment*, **583**, 280–291.

Chen J., de Hoogh K., Gulliver J., et al. (2019). A comparison of linear regression, regularization, and machine learning algorithms to develop Europe-wide spatial models of fine particles and nitrogen dioxide. *Environment International*, **130**, 104934.

Cheng Y., He K., Du Z., et al. (2015). Humidity plays an important role in the $PM_{2.5}$ pollution in Beijing. *Environmental Pollution*, **197**, 68–75.

Cheng G., Hu Y., Sun M., et al. (2019). Characteristics and potential source areas of aliphatic amines in PM2.5 in Yangzhou, China. *Atmospheric Pollution Research*, **11**(2).

Ding Y., Zhang M., Chen S., et al. (2019). The environmental Kuznets curve for $PM_{2.5}$ pollution in Beijing-Tianjin-Hebei region of China: A spatial panel data approach. *Journal of Cleaner Production*, **220**, 984–994.

Feng J., Yu H., Liu S., et al. (2017). $PM_{2.5}$ levels, chemical composition and health risk assessment in Xinxiang, a seriously air-polluted city in North China. *Environmental Geochemistry and Health*, **39**(5), 1071–1083.

Fu X., Wang X., Hu Q., et al. (2016). Changes in visibility with $PM_{2.5}$ composition and relative humidity at a background site in the Pearl River Delta region. *Journal of Environmental Sciences*, **40**: 10–19.

Gong T., Sun Z., Zhang X., et al. (2019). Associations of black carbon and $PM_{2.5}$ with daily cardiovascular mortality in Beijing, China. *Atmospheric Environment*, **214**, 116876.

Guo, X., Zhao, L., Chen, D., et al. (2018). Air quality improvement and health benefit of $PM_{2.5}$ reduction from the coal cap policy in the Beijing–Tianjin–Hebei (BTH) region, China. *Environmental Science and Pollution Research*, **25**(32), 32709–32720.

He Q., Gu Y. and Zhang M. (2020). Spatiotemporal trends of $PM_{2.5}$ concentrations in central China from 2003 to 2018 based on MAIAC-derived high-resolution data. *Environment International*, **137**, 105536.

Hou X., Zhu B., Kumar K.R., et al. (2019). Inter-annual variability in fine particulate matter pollution over China during 2013–2018: Role of meteorology. *Atmospheric Environment*, **214**, 116842.

Hough I., Just A.C., Zhou B., et al. (2020). A multi-resolution air temperature model for France from MODIS and Landsat thermal data. *Environmental Research*, **183**, 109244.

Hu J., Wang Y., Ying Q., et al. (2014). Spatial and temporal variability of $PM_{2.5}$ and PM_{10} over the North China Plain and the Yangtze River Delta, China. *Atmospheric Environment*, **95**, 598–609.

Jamil B. and Bellos E. (2019). Development of empirical models for estimation of global solar radiation exergy in India. *Journal of Cleaner Production*, **207**, 1-16.

Ji D., Yan Y., Wang Z., et al. (2018). Two-year continuous measurements of carbonaceous aerosols in urban Beijing, China: Temporal variations, characteristics and source analyses. *Chemosphere*, **200**, 191–200.

Ji D., Gao M., Maenhaut W., et al. (2019). The carbonaceous aerosol levels still remain a challenge in the Beijing-Tianjin-Hebei region of China: Insights from continuous high temporal resolution measurements in multiple cities. *Environment International*, **126**, 171–183.

Jin L., Berman J.D., Warren J.L., et al. (2019). A land use regression model of nitrogen dioxide and fine particulate matter in a complex urban core in Lanzhou, China. *Environmental Research*, **177**, 108597.

Lei Z., Jianjun W.U., Ruijing J., et al. (2016). Investigation of Temporal-Spatial Characteristics and Underlying Risk Factors of $PM_{2.5}$ Pollution in Beijing-Tianjin-Hebei Area. *Research of Environmental Sciences*.

Li N., Maesano C.N., Friedrich R., et al. (2019). A model for estimating the lifelong exposure to $PM_{2.5}$ and NO_2 and the application to population studies. *Environmental Research*, **178**, 108629.

Li M., Wang L., Liu J., et al. (2020). Exploring the regional pollution characteristics and meteorological formation mechanism of $PM_{2.5}$ in North China during 2013–2017. *Environment International*, **134**, 105283.

Liu K. and Ren J. (2019). Characteristics., sources and health risks of PM2.5-bound potentially toxic elements in the northern rural China. *Atmospheric Pollution Research*, **10**(5), 1621–1626.

Liang Z., Yang Y., Qian Z., et al. (2019). Ambient $PM_{2.5}$ and birth outcomes: Estimating the association and attributable risk using a birth cohort study in nine Chinese cities. *Environment International*, **126**, 329–335.

Ma J., Ding Y., Cheng J C P., et al. (2019). A temporal-spatial interpolation and extrapolation method based on geographic Long Short-Term Memory neural network for $PM_{2.5}$. *Journal of Cleaner Production*, **237**, 117729.

Pan S.C., Huang C.C., Chin W.S., et al. (2019). Association between air pollution exposure and diabetic retino-pathy among diabetics. *Environmental Research*, **181**, 108960.

Song Y., Zhang Y. and Dai W. (2011). $PM_{2.5}$ Sources and Their Effects on Human Health in China: Case Report. *Encyclopedia of Environmental Health*, **2011**, 606–613.

Sun X., Wang K., Li B., et al. (2020). Exploring the cause of $PM_{2.5}$ pollution episodes in a cold metropolis in China. *Journal of Cleaner Production*, **256**, 120275.

Tai A.P.K., Mickley L.J. and Jacob D.J. (2010). Correlations between fine particulate matter ($PM_{2.5}$) and meteorological variables in the United States: Implications for the sensitivity of $PM_{2.5}$ to climate change. *Atmospheric Environment*, **44**(32), 3976–3984.

Tayarani M. and Rowangould G. (2019). Estimating exposure to fine particulate matter emissions from vehicle traffic: Exposure misclassification and daily activity patterns in a large, sprawling region. *Environmental Research*, **182**, 108999.

Wang Z., Li Y., Chen T., et al. (2015a). Ground-level ozone in urban Beijing over a 1-year period: Temporal variations and relationship to atmospheric oxidation. *Atmospheric Research*, **164**, 110–117.

Wang G., Cheng S., Li J., et al. (2015b). Source apportionment and seasonal variation of $PM_{2.5}$ carbonaceous aerosol in the Beijing-Tianjin-Hebei Region of China. *Environmental Monitoring and Assessment*, **187**(3), 143.

Wang L., Li P., Yu S., et al. (2018). Predicted impact of thermal power generation emission control measures in the Beijing-Tianjin-Hebei region on air pollution over Beijing, China. *Scientific Reports*, **8**(1), 934.

Wang Z., Li Y., Chen T., et al. (2016). Science–policy interplay: improvement of air quality from 2008 to 2014 in Beijing and the scientific approach to achieve APEC blue. *Bulletin of the American Meteorological Society*, **97**(4), 553–559.

Wang Y., Chen S. and Yao J. (2019). Impacts of deregulation reform on $PM_{2.5}$ concentrations: A case study of business registration reform in China. *Journal of Cleaner Production*, **235**, 1138–1152.

Wu C.D., Zeng Y.T. and Lung S.C.C. (2018a). A hybrid kriging/land-use regression model to assess $PM_{2.5}$ spatial-temporal variability. *Science of the Total Environment*, **645**, 1456–1464.

Wu Y., Wang P., Yu S., et al. (2018b). Residential emissions predicted as a major source of fine particulate matter in winter over the Yangtze River Delta, China. *Environmental Chemistry Letters*, **16**, 1117–1127.

Xue T., Zheng Y., Tong D., et al. (2019). Spatiotemporal continuous estimates of $PM_{2.5}$ concentrations in China, 2000–2016: A machine learning method with inputs from satellites, chemical transport model, and ground observations. *Environment International*, **123**, 345–357.

Xie Y., Dai H., Zhang Y., et al. (2019). Comparison of health and economic impacts of $PM_{2.5}$ and ozone pollution in China. *Environment International*, **130**, 104881.

Xie X., Ai H. and Deng Z. (2020). Impacts of the scattered coal consumption on $PM_{2.5}$ pollution in China. Journal of Cleaner Production, **245**, 118922.

Yan D., Lei Y., Shi Y., et al. (2018). Evolution of the spatiotemporal pattern of $PM_{2.5}$ concentrations in China–A case study from the Beijing-Tianjin-Hebei region. *Atmospheric Environment*, **183**, 225–233.

Yang X., Liang F., Li J., et al. (2020). Associations of long-term exposure to ambient $PM_{2.5}$ with mortality in Chinese adults: A pooled analysis of cohorts in the China-PAR project. *Environment International*, **138**, 105589.

Ye Z., Guo X., Cheng L., et al. (2019). Reducing $PM_{2.5}$ and secondary inorganic aerosols by agricultural ammonia emission mitigation within the Beijing-Tianjin-Hebei region, China. *Atmospheric Environment*, **219**, 116989.

Yi Y., Zhou X., Xue L., et al. (2018). Air pollution: formation of brown, lighting-absorbing, secondary organic aerosols by reaction of hydroxyacetone and methylamine. *Environmental Chemistry Letters*, **16**, 1083–1088.

Young M.T, Bechle M.J., Sampson P.D., et al. (2016). Satellite-based NO_2 and model validation in a national prediction model based on universal kriging and land-use regression. *Environmental Science & Technology*, **50**(7), 3686–3694.

Yu S., Zhang Q., Yan R., et al. (2014). Origin of air pollution during a weekly heavy haze episode in Hangzhou, China. *Environmental Chemistry Letters*, **12**(4), 543–550.

Yue H., Huang Q., He C., et al. (2020). Spatiotemporal patterns of global air pollution: a multi-scale landscape analysis based on dust and sea-salt removed $PM_{2.5}$ data. *Journal of Cleaner Production*, **252**, 119887.

Zhang Z., Wang W., Cheng M., et al. (2017). The contribution of residential coal combustion to $PM_{2.5}$, pollution over China\"s Beijing-Tianjin-Hebei region in winter. *Atmospheric Environment*, **159**, 147–161.

Zhang J., Liang S., Ning R., et al. (2020). $PM_{2.5}$-induced inflammation and lipidome alteration associated with the development of atherosclerosis based on a targeted lipidomic analysis. *Environment International*, **136**, 105444.

Zhao T., Yang L., Yan W., et al. (2017). Chemical characteristics of PM_1/$PM_{2.5}$ and influence on visual range at the summit of Mount Tai, North China. *Science of The Total Environment*, **575**, 458–466.

Zhao X., Zhou W., Han L., et al. (2019). Spatiotemporal variation in $PM_{2.5}$ concentrations and their relationship with socioeconomic factors in China's major cities. *Environment International*, **133**, 105145.

Zheng H., Zhao B., Wang S., et al. (2019). Transition in source contributions of $PM_{2.5}$ exposure and associated premature mortality in China during 2005–2015. *Environment International*, **132**, 105111.

Zhu Y., Huang L., Li J., et al. (2018). Sources of particulate matter in China: Insights from source apportionment studies published in 1987–2017. *Environment International*, **115**, 343–357.